

المؤتمر الجزائري الثالث للجيوسينتيتيك 3rd Algerian Geosynthetics Congress 3^{éme} Congrès Algérien des Géosynthétiques



ENSTP, Kouba Alger le 21 & 22 septembre 2025

Numerical Analysis of Back-to-Back Geogrid-Reinforced railway subgrade during and after construction.

Abdelkader Dram* 1, Imad Eddine Debbabi 2, Mohamed Lahlali3

^{1,2} Department of Civil Engineering and Hydraulic, NMISSI Laboratory, Biskra University, BP 145, Biskra 07000, Algeria, Email: abdelkader.dram@univ-biskra.dz.

Abstract. This paper estimates the performance evaluation of speared, and overlapped geogrid reinforced back-to-back mechanically stabilized earth walls supporting the railway tracks at bridge approaches. A numerical model for four cases was developed to analyze study was also carried out on varying W= (1.4;2 and 3H), LR =0.2H. Train bogie load was used as a loading condition. Lateral earth pressures, vertical deformations of walls, geogrid strain, maximum tensile force developed in the geogrid for all the cases were investigated and discussed in detail. Geogrid arrangements were found to be critical in reducing the wall displacement. The overlapping length of the geogrid resulted in lesser deformation compared to the speared geogrid.

Keywords: Back-to-back walls, Numerical analysis, Geosynthetics; Geosynthetic reinforced soil; Mechanically stabilized earth.

1. Introduction

Back-to-back mechanically stabilized earth (BBMSE) walls are widely used in various projects. In the Federal Highway Administration (FHWA) design guide lines on reinforced soil walls (Berg et al. (2009)), recommendations on the lateral earth pressures against BBMSE walls under static loading were highlighted. However, numerical model studies on the seismic behavior of BBMSE are very limited or nonexistent.

Due to superior performance of reinforced-soil structure compared to that of a conventional retaining wall, especially in seismic areas, the seismic behavior of these structures has been researched widely e.g., Bathurst and Hatami (1998); Rowe and Ho (1998); Hatami and Bathurst (2000); Bathurst et al. (2002); Watanbe et al.

(2003); Ling et al. (2004); Siddharthan et al. (2004); El-Emam and Bathurst (2005); Hatami and Bathurst (2005); Ling et al. (2005); Nova-Roessig and Sitar (2006); El-Emam and Bathurst (2007); Fakharian and Attar (2007); Latha and Krishna (2008); Bhattacharjee and Krishna (2015); Murali Krishna and Bhattacharjee (2017); Yazdandoust (2018a, 2018b and 2019).

In the FHWA design guidelines [Berg et al. (2009)], two cases were presented to estimate the lateral pressures at the end of the reinforced zone for external stability calculations, based on the distance of two back-to-back or opposing walls, D (Figure 1). For Case I, walls are designed as independent walls if they are sufficiently far away, i.e., with D greater than H × $\tan(45^{\circ}-\phi/2)$. While for Case II, no active earth thrust from the backfill on the walls be taken into account for the external stability calculations if D=0 and the overlap length of the reinforcements from the two walls, LR, is greater than 0.3H, where H is the height of the wall. Till date, there are no formal design guidelines for closely spaced back-to-back MSE walls (i.e., $0 < D < H × \tan(45^{\circ}-\phi/2)$). The above guidelines are valid for static loading conditions or in areas where the seismic horizontal accelerations at the foundation level are less than 0.05g [Berg et al. (2009)].

In the present study, A numerical model for four cases was developed to analyze study was also carried out on varying W= (1.4;2 and 3H), LR =0.2H. Train bogie load was used as a loading condition. Lateral earth pressures, vertical deformations of walls, geogrid strain, maximum tensile force developed in the geogrid for all the cases were investigated and discussed in detail. Geogrid arrangements were found to be critical in reducing the wall displacement. The overlapping length of the geogrid resulted in lesser deformation compared to the speared geogrid we will seeing.

2. Numerical modeling

3.2 Finite Element Modeling

In the present study, a finite element-based program, PLAXIS 2D, was used to develop a plane-strain model to analysis of the BBMSE supporting the railway walls. A 6 m-high wall resting on a 2 m-thick soil foundation and 0.3m thick ballast above the builder was considered. Figure 3.1 represents a finite element model of back-to-back MSE walls. For this, a overlapped model is chosen with of LR/H = 0.2 and a three models speared ratio in W/H= (1.4; 2 and 3H) the length of the reinforcements for the two walls was considered as LR = 4.2 m (the typical rebar length recommended by FHWA design guidelines (FHWA 2009), i.e. LR=0.7H).

3.2.1 Soil Proprieties

The foundation soil was modeled as Mohr-Coulomb material with very high deformation modulus (E=200 MPa) to simulate it as a rigid material. The model involves six input parameters, namely, deformation modulus (E), Poisson ratio (v), cohesion (c), friction angle (φ), and dilatancy angle (ψ). Table 3.1 presents the values of the material properties considered in the study. The soil-reinforcement interaction was modeled by relating the nonlinear elastic behavior of the soil to the linear elastic response of the reinforcement. For this purpose, the

geogrids are selected from the elastoplastic elements with stiffness and tensile strength. The interaction between the geogrid and soil was simulated using interface element.

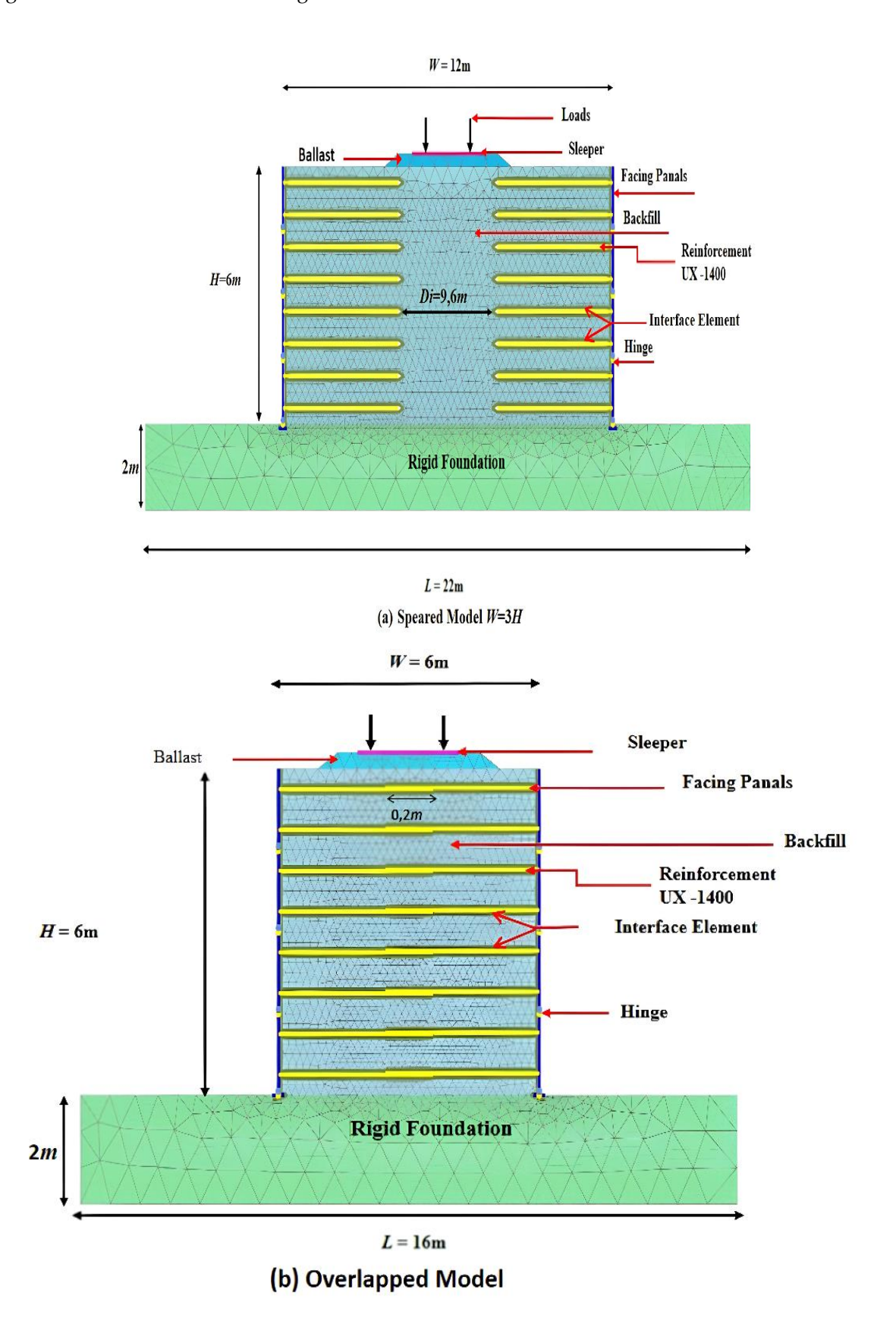


Figure 3.1 Finite element models of back-to-back MSE walls.

Table 3. 1. Material properties used in numerical simulations (Benmebarek el al. 2016).

Material	Symbol	Unit	Reinforced backfill	Foundation	Ballast
				soil	
Unit weight	γs	KN/m3	18	22	21
Angle of shearing resistance	ф	degrees	35	30	35
Dilatancy angle	Ψ	degrees	5	0	5
Deformation modulus	E	KPa	30×103	200×103	30×103
Cohesion	c	KPa	0	200	30
Poisson's ratio	V	-	0.3	0.2	0.3

Table 3. 2. Reinforcement properties.

Identification	Model	Ultimate	tensile	Allowable	tensile	Axial
		strength		strength, Ta		stiffness
Uniaxial geogrid	Elastoplastic	70 KN/m		25.6 KN/m	1	1,100 KN/m

3.2.2 Reinforcement

Table 3.2 gives the properties of the reinforcement - uniaxial geogrid (UX-1400 type). Geogrids were placed at typical pacing of 0.75 m (AASTHO 2012). The well-known segmental precast concrete panels were considered in the current study to simulate the wall. Each wall contains 4 segmental concrete panels of 1.5 m in width and height and 0.14 m in thickness.

3.2.3 Facing: Precast Panels

The concrete panel facia was modeled as a linear-elastic material. In the present model, the facing panel was hinged to a horizontal plate which is 0.5m embedded in the foundation soil. Hence the panel had the flexibility to move in horizontal direction. However, the panel cannot be moved in vertical direction. The boundary condition applied in the model, simulates the real situation of embedment with nominal footing at the bottom of the concrete panel. Hence, nominal lateral displacements can be expected in the real time scenario for the seismic loading. In the finite element model, the properties of the facing panel were defined by its young's

modulus, E = 25 GPa and the unit weight γ c= 23.5 KN/m3. Table 3.3 gives the properties of the facia considered in the study.

Table 3. 3. Material properties of concrete panel facing elements and sleeper.

Identification	Elastic stiffness	Flexural rigidity	Thickness	Weight of panel	Poisson
	(EA)	(EI)	(d)	(Wc)	ratio (vc)
Concrete	3.5×106 KN/m	5,717 KN/m2	0.14 m	3.29KN/m	0.2
panel facing					
Sleeper	10.5×106 KN/m	7,875 KN/m2	0.30 m	7.5 KN/m	0.2

3.2.4 Interface properties

The interaction between the facing panel elements and the backfill and between the backfill and reinforcement were modeled by using interface elements (refer to Figure 3.1). A partially rough interface was considered, such that the interface parameter, Rinter, was equal to $\tan \delta' / \tan \phi$, where interface friction angle $\delta' = 23.0^{\circ}$ and backfill friction angle $\phi = 35^{\circ}$. For the present study, the interface strength was reduced by using the strength reduction factor = 0.60 < 1 in these analyses.

3.4 Results and Discussions

3.4.1 Displacements of the wall

Figure 3.2 shows the differences in maximum displacement at the interface for different successive MSE walls (BBMSEWs) under the effect of rail load. Comparison of three separate variable distance D models for different W ratio (1.4; 2 and 3H) with the overlap model of length reinforcement distances (LR = 0.2H). The results indicate that the staggered walls on either side of the BBMSEWs significantly reduce the lateral displacements. On the other hand, the walls separated from each other cause the displacement to be almost the same for W/H = 3.0 and 2.0. The highest offset is at W/H = 1.4, however, increasing the aspect ratio from 1.4 to 3.0 increases the maximum horizontal offset. These results were justified because successive walls do not interact with each other, therefore, the two successive walls must operate independently when the walls overlap LR = 0.2H.

3.4.2 Earth pressures behind wall.

Figure 3.3 depicts the lateral earth pressure behind the wall, the lateral earth pressure. Accordingly, the earth pressures from the numerical model were presented and compared with those the active Rankine. However, the lateral earth pressure decreases in the overlapping model LR=0.2H and increases in the separate models

when compared with the overlapped model which means are the overlapped better than separate (W=1.4; 2 and 3H).

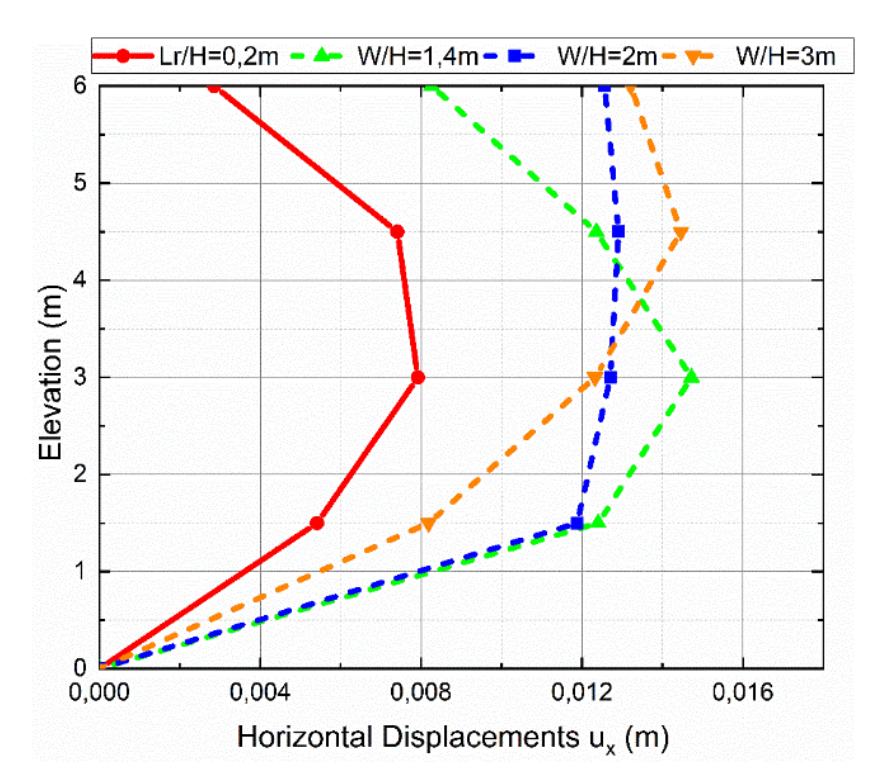


Figure 3.2 Horizontal Displacements UX for the wall.

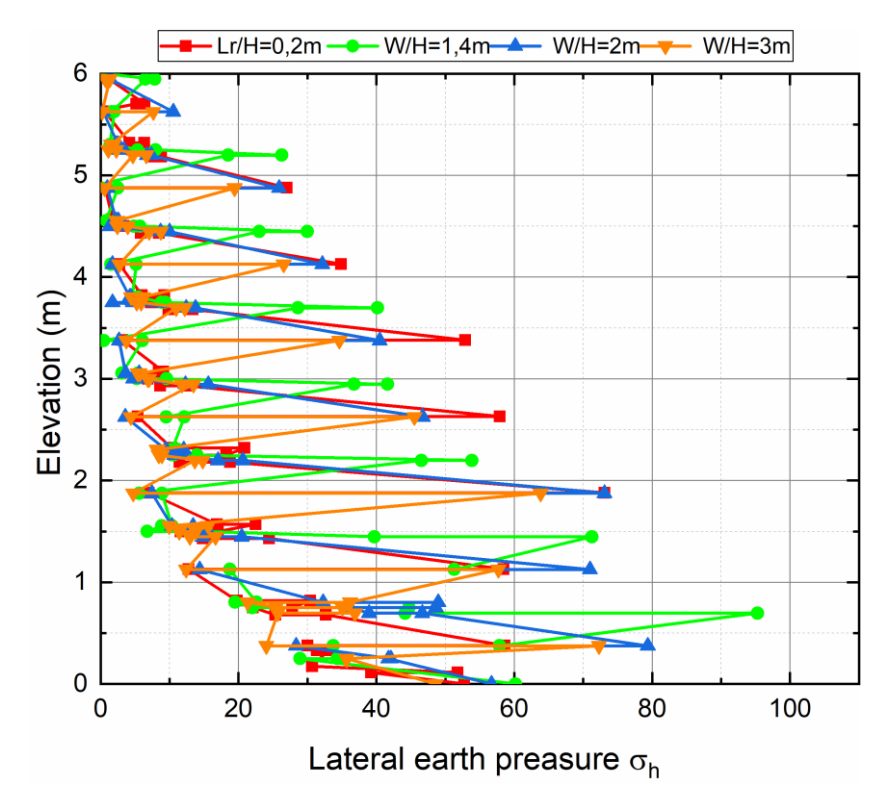


Figure 3.3 Earth pressure at the facing

3.4.3 Distribution of tensile force in reinforcements

Figure 3.4 shows the tensile forces along the geogrid layers in the overlapped model and speared models at the end of construction. The maximum tensile forces in the geogrid layers with the product of soil unit weight, the geogrid vertical and horizontal intervals (SV and SH), and the wall height (H). The results indicate that near the wall facing, the tensile forces in both the overlapped and speared reinforcements increased with depth due to the effect.

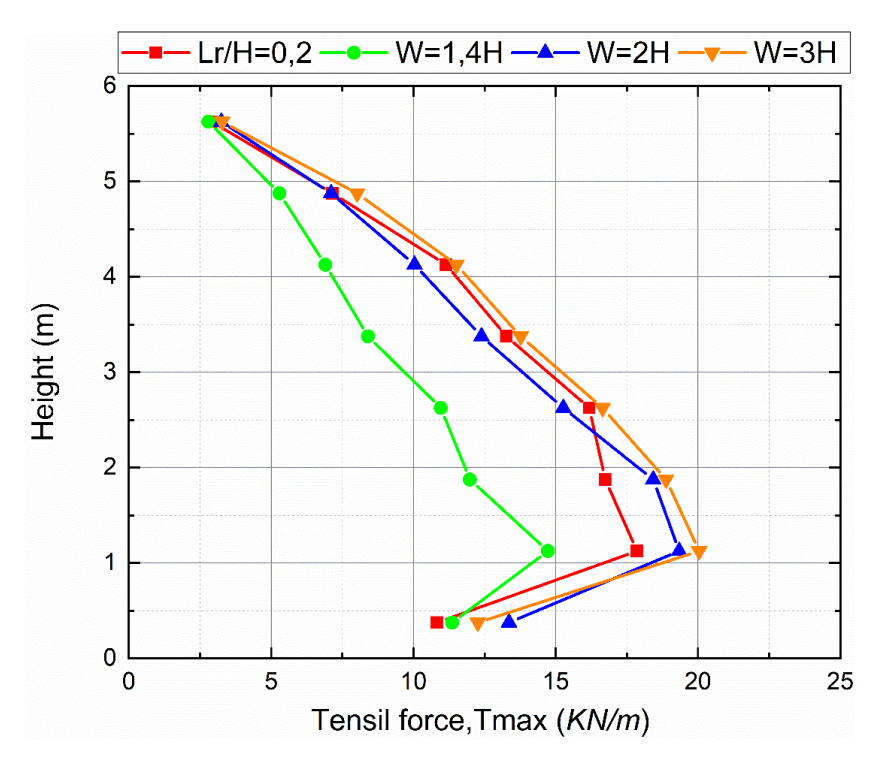


Figure 3.4 Maximum tension in reinforcement.

3.4.4. Tensile Forces in Geogrids length

Figure 3.5 shows the maximum tensile forces in the geogrid layers were with the product of soil unit weight (γ) , the geogrid vertical intervals (SV) and the wall height (H). The results indicate that the bottom reinforcements experience the maximum force compared to those of the top reinforcements of the facing. As expected from previous results, the high tensile force in the reinforcements the base of the wall was the result of both high overburden stress and a retaining effect due to geogrid reinforcements. As expected from previous results, in the overlapped model the tensile loads become less than the separate models (W=1.4; 2 and 3H).

3.4.5 Vertical deformation

Figure 3.6 shows the vertical deformation for the Models of (LR= 0.2/H and W/H = 2). For the geogrid spacing of 0.75 m, the vertical deformation was observed to be maximum at the zone near the point of application of railway load compared in both cases. This may be because; below the points of application of loading, the reinforcement is missing and the displacement is maximum in the middle and spreading towards the surrounding area. The results indicate that the overlapped model has less and regular deformation than the speared model.

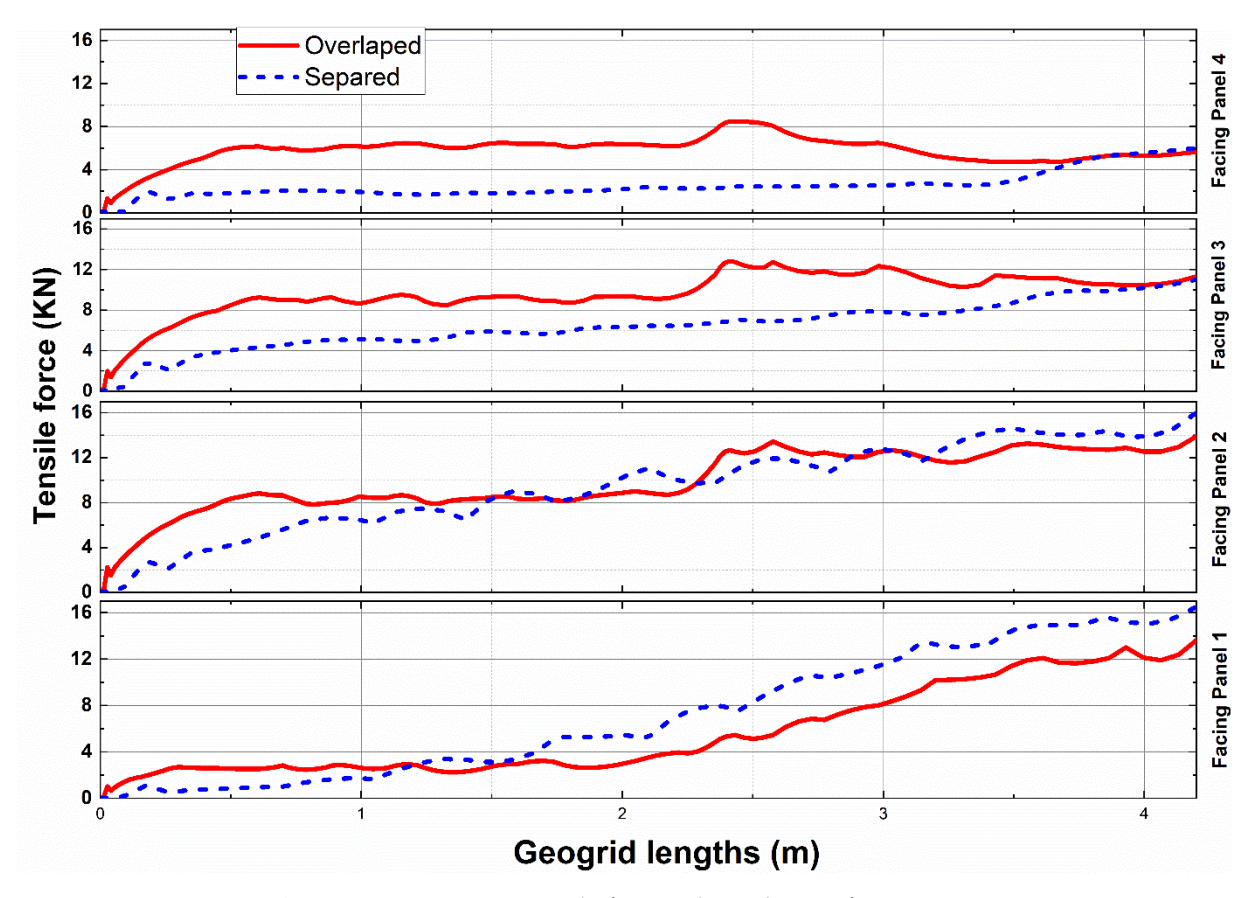


Figure 3.5 Maximum tensile forces along the reinforcements.

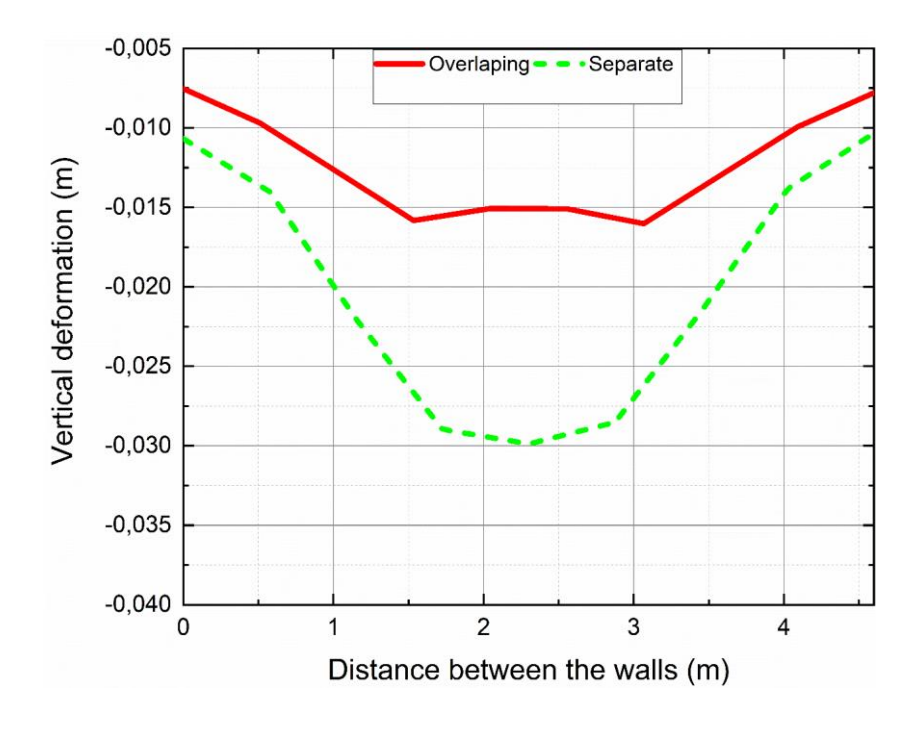


Figure 3.6 Vertical deformation between the walls

3.4.6 Load vs settlement response of back-to-back MSE wall model

In FE analysis more significant deformations have been observed in the speared walls models compared to the overlapped model. Lesser wall displacement was observed for overlapped case. Load settlement responses of all the models are shown in Figure 3.7 In both the cases, the failure load was defined at the point on the load-settlement curve when the slope practically reached zero or any steady minimum value. The load settlement responses observed from the model tests and those predicted by the numerical studies were very similar.

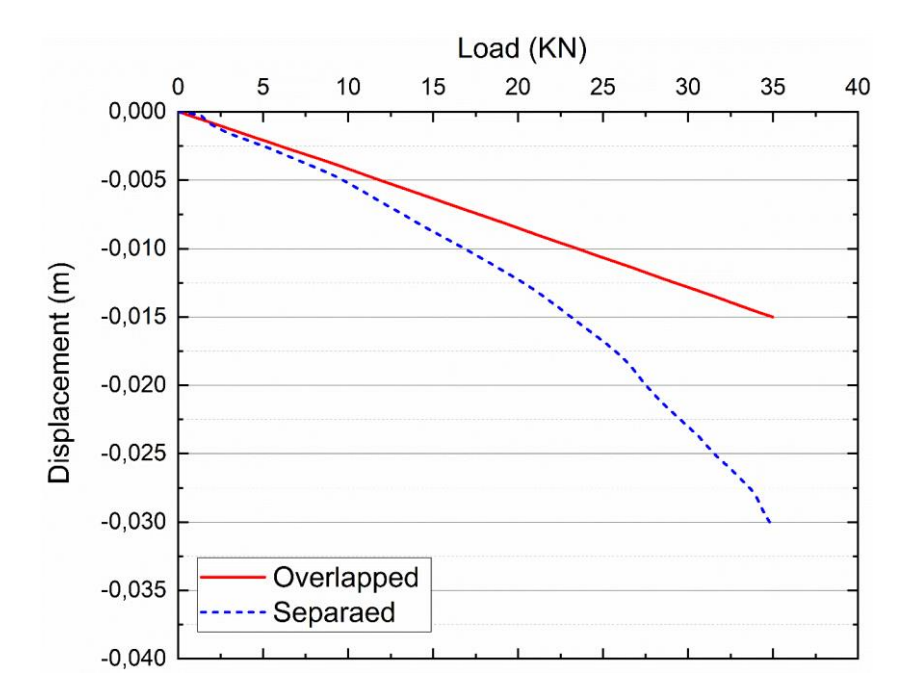


Figure 3.7 The load settlement responses observed from the model tests LR=0.2H and W = 2H.

3.4.7 Mechanisms of Potential Failure

Figure 3.8 shows the distribution of plastic points and of shear strain increment contours in both overlapped and speared walls at the end of the railway load. The Mohr–Coulomb plastic points indicate that the Coulomb failure is reached for these points. Shear strain increment contours were used to visualize more clearly the localization of the potential failure mechanism than the distribution of plastic points. For the four models, shear strain bands were developed from the bottom of the two cases and spread with an angle close to the angle of shearing resistance of the backfill. In the case of unconnected walls, the interception of shear bands from the two walls created a triangular failure zone in the middle top of the BBMSE walls.

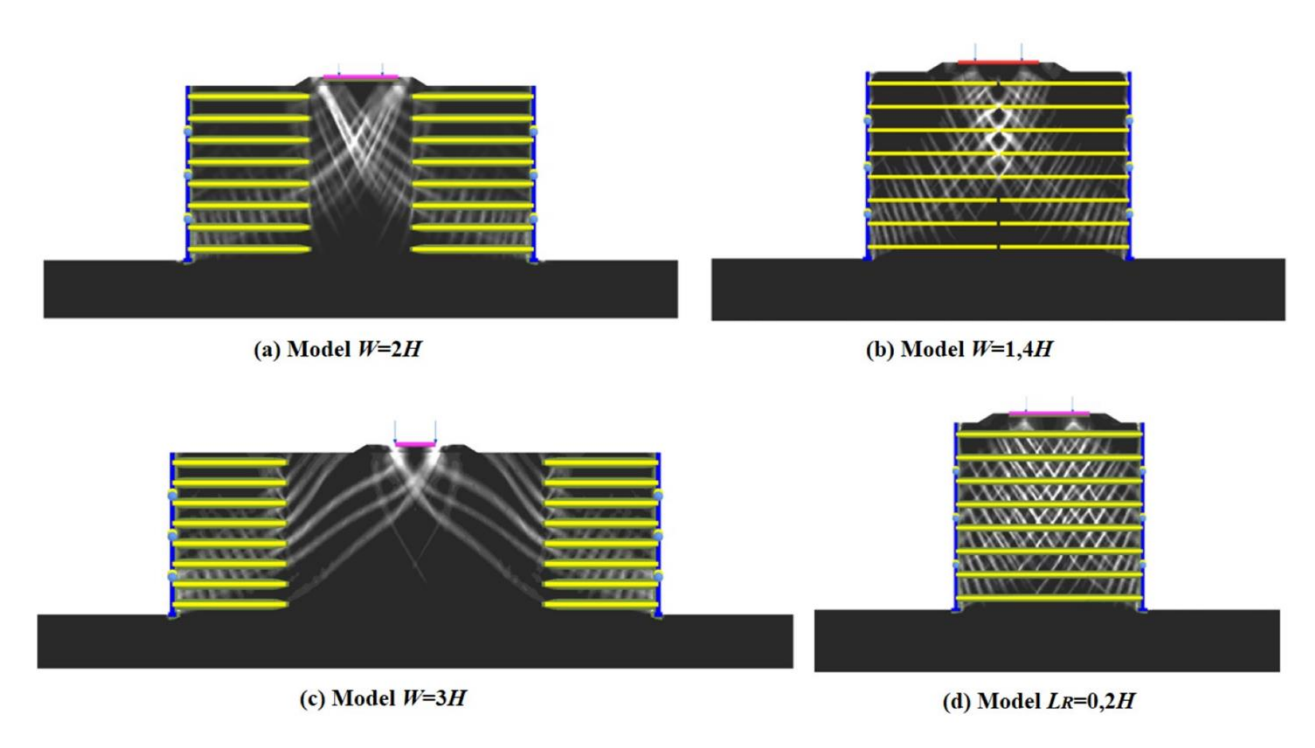


Figure.3.8 The distribution of plastic points and of shear strain increment contours in both overlapped and speared.

3.5 Conclusions

The study findings demonstrate that utilizing an overlapped model can effectively minimize lateral displacements in BBMSEW. On the other hand, when walls are completely separated from each other, it leads to the maximum lateral displacements, making the overlapped reinforcing better for BBMSEW structures under railway conditions.

References

- 1. AASTHO. 2012. AASHTO LRFD Bridge design specifications, 6th edn. American Association of State Highway and Transportation Officials (AASHTO), Washington DC.
- 2. Anastasopoulos, I., T. Georgarakos, V. Georgiannou, V. Drosos, and R. Kourkoulis. 2010. "Seismic performance of bar-mat reinforced soil retaining wall: Shaking table testing versus numerical analysis with modified kinematic hardening constitutive model." Soil Dynamics and Earthquake Engineering. 30(10): 1089-1105. https://doi.org/10.1016/j.soildyn.2010.04.020.
- 3. Anubhav, S., and P. K. Basudhar. 2011. "Numerical modelling of surface strip footings resting on double-faced wrap-around vertical reinforced soil walls." Geosynthetics International. 18 (1): 21–34. https://doi.org/10.1680/gein.2011.18.1.21.
- 4. Bathurst, R. J., and K. Hatami. 1998. "Seismic response analysis of a geosynthetic-reinforced soil retaining wall." Geosynthetics International. 5(1–2): 127–166. https://doi.org/10.1680/gein.5.0117.
- 5. Bathurst, R. J., K. Hatami, and M. C. Alfaro. 2002. "Geosynthetic -reinforced soil walls and slopes seismic aspects." Geosynthetics and their applications, S. K. Shukla, ed., Thomas Telford Ltd., London, UK, 327–392.

- 6. Benmebarek, S., S. Attallaoui, and N. Benmebarek. 2016. "Interaction analysis of back-to-back mechanically stabilized earth walls." Journal of Rock Mechanics and Geotechnical Engineering. 8(5): 697–702. https://doi.org/10.1016/j.jrmge.2016.05.005.
- 7. Benmebarek, S., and M. Djabri. 2017a. "FE Analysis of Back-to-Back Mechanically Stabilized Earth Walls Under Cyclic Harmonic Loading." Indian Geotechnical Journal. 48 (3): 498-509. https://doi.org/10.1007/s40098-017-0269-z.
- 8. Benmebarek, S., and M. Djabri. 2017b. "FEM to investigate the effect of overlapping-reinforcement on the performance of back-to-back embankment bridge approaches under self-weight." Transportation Geotechnics. 11: 17–26. https://doi.org/10.1016/j.trgeo.2017.03.002.
- 9. Berg, R. R., B. R. Christopher, and N. C. Samtani. 2009. Vol. I of Design and construction of mechanically stabilized earth walls and reinforced soil slopes. Geotechnical Engineering Circular No. 011, FHWA-NHI-10-024. Washington, DC: FHWA.
- 10. Bhattacharjee, A., and A. Krishna. 2015. "Strain behavior of backfill soil in rigid faced reinforced soil walls subjected to seismic excitation." International Journal of Geosynthetics and Ground Engineering.1(2):14. https://doi.org/10.1007/s40891-015-0016-4.
- 11. Brinkgreve, R. B. J. 2018. PLAXIS 2D Reference Manual 2018, Delft University of Technology and PLAXIS by The Netherlands.
- 12. Djabri, M., and S. Benmebarek. 2016. "FEM analysis of back-to-back geosynthetic-reinforced soil retaining walls." International Journal of Geosynthetics and Ground Engineering. 2 (3): 26. https://doi.org/10.1007/s40891-016-0067-1.
- 13. El-Emam, M., and R. J. Bathurst. 2005. "Facing contribution to seismic response of reduced-scale reinforced soil walls." Geosynthetics International. 12 (5): 215–238. https://doi.org/10.1680/gein.2005.12.5.215.
- 14. El-Emam, M., and R. J. Bathurst. 2007. "Influence of reinforcement parameters on the seismic response of reduced-scale reinforced soil retaining walls." Geotextiles and Geomembranes. 25 (1): 33–49. https://doi.org/10.1016/j.geotexmem.2006.09.001.
- 15. El-Sherbiny, R., E. Ibrahim, and A. Salem. 2013. "Stability of back-to -back mechanically stabilized earth walls." In Geo-Congress 2013: Stability and Performance of Slopes and Embankments III, Geotechnical Special Publication 231, edited by C. Meehan, D. Pradel, M. A. Pando, and J. F. Labuz, 555–565. San Diego, CA: ASCE.
- 16. Fakharian, K., and I. Attar. 2007. "Static and seismic numerical modeling of geosynthetic-reinforced soil segmental bridge abutments." Geosynthetics International. 14(4): 228–243. https://doi.org/10.1680/gein.2007.14.4.228.
- 17. A. Mecke, I. Lee, J.R. Baker jr., M.M. Banaszak Holl, B.G. Orr, Eur. Phys. J. E 14, 7 (2004)
- 18. M. Ben Rabha, M.F. Boujmil, M. Saadoun, B. Bessaïs, Eur. Phys. J. Appl. Phys. (to be published)
- 19. Luigi T.De Luca, Propulsion physics (EDP Sciences, Les Ulis, 2009)
- 20. F. De Lillo, F. Cecconi, G. Lacorata, A. Vulpiani, EPL, 84 (2008).